

# Velocity Measurements in a Turbulent Centerbody Diffusion Flame

Larry A. Roe\*

*Virginia Polytechnic Institute and State University, Blacksburg, Virginia*  
and

Charles L. Proctor, Jr.†

*University of Florida, Gainesville, Florida*

A two-color, two-component, laser Doppler anemometer was used to measure mean velocities, velocity fluctuations, Reynolds shear, and correlation coefficients for the axial and radial directions in a centerbody turbulent diffusion burner exhausting into free air. Both fuel composition and flow rates were varied. Mean velocities and turbulent fluctuations obtained by a time-weighted data analysis technique were found not to differ significantly from particle averaged values. Comparisons between reacting and nonreacting cases showed the reaction to increase the axial and radial extent of the separation region, increase the axial turbulent fluctuations, and increase the shear stress. Increases in fuel flow beyond a very lean flame did not significantly affect the velocity parameters. The turbulence was found to be nonisotropic, and regions of zero shear were observed in regions of nonzero turbulent kinetic energy, both inconsistent with typical eddy viscosity and  $k-\epsilon$  turbulence model assumptions.

## Introduction

THE flowfield in the wake of a centerbody diffusion burner was mapped using a two-component laser Doppler anemometer (LDA) as part of a soot formation study for application to gas turbine combustors. The production of soot in gas turbine engines is of concern as it is indicative of incomplete combustion, reduces the hot-section life due to increased radiative heat loadings, and, especially for military applications, increases both the visible and infrared signatures of the aircraft.

In this type burner, which represents processes occurring in the primary reaction zone of a gas turbine combustor, the air-flow is separated behind the centerbody, and the reaction occurs in the recirculating wake region. Any attempt to model the chemical processes occurring in the reaction zone must account for the flow patterns in this area, as the initial generation of particulates and their eventual destruction depend on the flow path through whatever chemical and thermal fields exist.

This paper first lists the pertinent operating parameters of the LDA system and describes the centerbody burner. Comparisons of the average flowfields in the recirculating zone for different fuel conditions are then made. The influence of reaction on the axial and radial components of the turbulent fluctuations, Reynolds shear, and turbulence correlation coefficient are presented, and conclusions are drawn. The velocity notation of Hinze<sup>1</sup> is used throughout.

## Laser Doppler Anemometer

The LDA system was essentially a TSI, Inc., Model 9100-7 with minor alterations. It used a four-watt, argon-ion laser operating in the multiline mode at a total output power level of 600 mW. The burner radial (horizontal) component of velocity was measured with the 514.5 nm green line at a fringe

spacing of 1.89 microns; a TSI 1990A counter provided the frequency measurement. The axial (vertical) component used the 488 nm blue line, a 1.82 micron fringe spacing, and a TSI 1980 counter. The probe volume had a length of approximately 1.5 mm and a diameter of approximately 0.5 mm. Collection was in the backscatter direction. Effective downmixed Bragg shift frequencies of 10 MHz were used for both components.

Eight Doppler cycles were counted, and data comparison was used at a 7% level. The component coincidence window was set at 1.2 millisecond to achieve an acceptably high data rate. The time between data points (TBD) feature was used to provide a temporal history of the flow; coincident frequency data and TBD information were transmitted to a PDP-11/34A minicomputer via a direct memory access data link. Velocity data were recorded at each of 45 spatial locations and stored on disk to allow for different data reduction techniques to be applied to the same data. A series of repeated measurements at a fixed location and fuel rate, with the number of recorded velocity realizations ranging from 256–2048, was used to establish expected accuracies in the mean velocities, turbulence components, and correlations. For the test data, 512 correlated velocity pairs were recorded at each spatial location.

The analysis and interpretation of LDA data require consideration of the manner in which the velocity measurements were acquired and averaged. In a report of the special panel on statistical particle bias problems in laser anemometry held during the Second International Laser Anemometry Symposium (1985), Edwards<sup>2</sup> summarizes the panel's opinions on the acquisition and treatment of LDA data. Although not all of these recommendations could be followed in this test program, the points raised in the report will be addressed.

Stored data rates in the recirculating region of the flowfield typically ranged from 20–500 Hz with a stored data point consisting of a coincident pair of radial and axial velocity realizations. The data acquisition capability of the interface system is much faster than this; therefore the validation rate can be considered to range over the same values. The trigger rate is not an available item of data with this system, and particle arrival rate is indeterminate due to the highly separated nature of the flowfield with the bulk of the injected seed not entering the recirculation zone. Although the Taylor time microscale required for a numerical calculation of data density was not determined, the validation rates would be expected to produce results in the low data density region.

Received Nov. 7, 1988; revision received April 15, 1989. Copyright © 1989 American Institute of Aeronautics and Astronautics, Inc. All rights reserved.

\*Assistant Professor, Department of Mechanical Engineering. Member AIAA.

†Associate Professor, Department of Mechanical Engineering. Member AIAA.

Angle bias was minimized by the utilization of 40 MHz Bragg cells on one beam of each component pair, creating in both cases effective fringe velocities on the order of 75 m/s, well in excess of the maximum fluid velocity of 15 m/s. Filter bias is not expected to be a difficulty as the filter settings utilized (1 kHz low limit, 30 or 50 MHz high limit) are well outside the observed data range of 6–23 MHz for the shifted doppler frequencies.

Velocity bias is a more difficult question to address. The panel report provided no unqualified recommendation for elimination of velocity bias in low data density measurements. Since TBD information was acquired and stored on disks with the individual particle velocities, it was possible to investigate the differences between particle averages and TBD-weighted average velocities.

Propene (propylene) data at an air/fuel ratio of 6000 was chosen as the test case. Particle averages were obtained by simply averaging the individual realizations with no accounting for the time required to obtain the measurement or the time between measurements. For comparison, a sample and hold type of biasing correction was implemented in the data analysis software to produce TBD-weighted statistics. This scheme multiplied each velocity by the time interval until the next stored data point, summed these weighted velocities and divided by the total of all interarrival times. This technique was recommended without qualification for high data densities, but its utilization for low or intermediate data densities was not addressed by the panel.

Deviations between results obtained using the two averaging techniques were calculated for the parameters of interest and averaged over all 45 locations in the spatial matrix. For the mean velocities, the average difference between the direct particle average (unweighted results) and TBD-weighted average was 0.090 m/s for the radial component and 0.102 m/s for the axial. The uncertainty in each component of the mean velocities, as obtained from the series of measurements at a fixed location and fuel rate, is approximately 0.25 m/s, or 2% of the maximum flow velocity. The difference between the two averaging techniques is therefore within the expected accuracy of the data.

The effects of weighting also did not significantly affect the calculation of turbulent fluctuations, with average differences of 0.068 m/s radial and 0.106 m/s axial observed between unweighted and weighted data. The expected accuracy of the data is 0.15 m/s, which indicates that the difference between results obtained from the two statistical treatments is again within the expected accuracy range of the data. The Reynolds shear results are not weighted, as the bias panel specifically advised against applying temporal corrections to cross-correlated parameters due to a lack of a suitable data base; whereas while

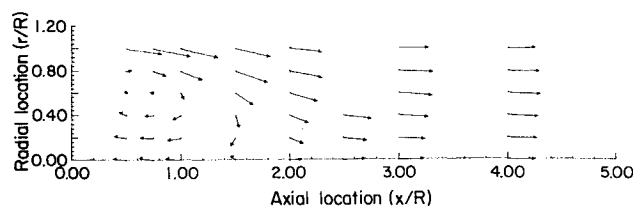


Fig. 2 Velocity vector plot for no fuel jet.

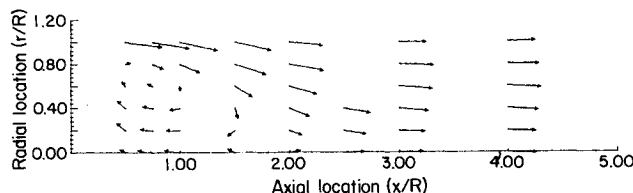


Fig. 3 Velocity vector plot for nitrogen at  $a/f = 400$ .

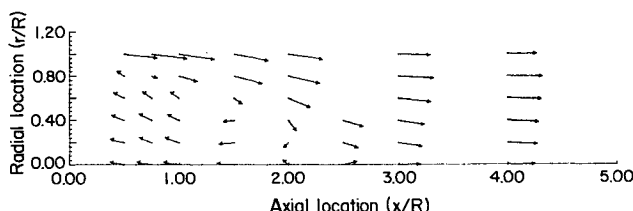


Fig. 4 Velocity vector plot for propylene at  $a/f = 6000$ .

the treatment of the correlation coefficient has something of a mixed nature as the stress in the numerator ( $-\overline{uv}$ ) is unweighted while the denominator ( $\overline{u'v'}$ ) is weighted.

#### Burner and Peripheral Systems

The burner used for this evaluation was a nonpremixed, centerbody type exhausting into free air. This design provides an intermediate model between simple, flat-flame type burners and actual gas turbine combustors. The apparatus is similar to devices used by numerous other researchers<sup>3-12</sup> and is identical to the burner used for soot particle distribution measurements by Touati.<sup>13</sup> Unlike several of the referenced designs, it exhausts into free air directly downstream of the centerbody, providing virtually unlimited optical access to the entire flowfield.

Figure 1 shows the burner assembly, coordinate system, and typical luminous region of the reaction zone. In addition to the strong flowfield generated by the annular airflow, the burner and supporting traverse table were surrounded by an acrylic enclosure to shield the measurement region from influence by air movement in the test facility. The air from the fluidized bed seeder entered the plenum and was mixed with the main combustion air. The fuel was unseeded; earlier investigations with this same burner (Proctor et al.<sup>3</sup>) and the results of Lightman et al.<sup>4</sup> showed no significant changes in mean-flow pattern or turbulence levels with the addition of fuel seeding. Schefer et al.<sup>5</sup> did observe sensitivity to fuel seeding; however, the contribution of the fuel flow to the overall recirculating flowfield was approximately an order of magnitude higher than in the studies presented here as a result of a comparable centerbody geometry, comparable air and fuel velocities, but a fuel jet area 15 times as large. Elimination of fuel seeding thus avoided plugging of the fuel nozzle, a 1.37 mm diam conical type designed for oil burner applications. Aluminum oxide particles of nominal 0.3  $\mu$  diam were used for seeding. Extractive sampling of seed particles from the measurement regions was not attempted.

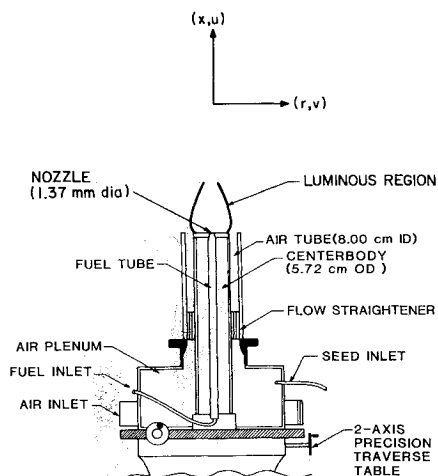


Fig. 1 Centerbody burner.

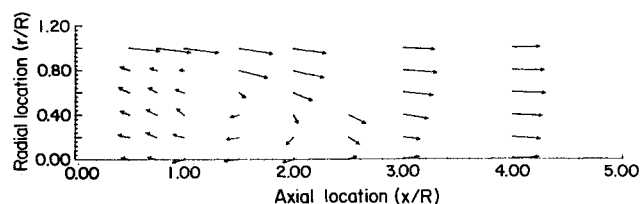


Fig. 5 Velocity vector plot for isobutene at  $a/f=800$ .

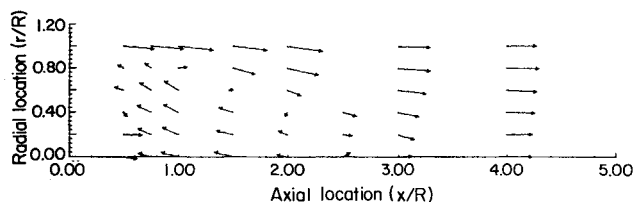


Fig. 6 Velocity vector plot for butene-nitrogen 1:1 mix at  $a/f=400$ .

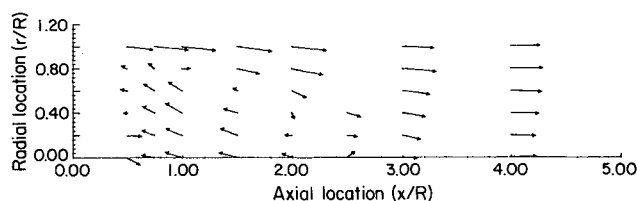


Fig. 7 Velocity vector plot for butene-nitrogen 2:1 mix at  $a/f=400$ .

The airflow rate was fixed for all tests and corresponded to an average annular velocity of 14 m/s. The fuel flow rates yield calculated velocities as high as 47 m/s for the reacting flows and 63 m/s for the nonreacting nitrogen flow when the calculations are based on the nozzle diameter; however, as the near-nozzle region was not of primary interest and fuel penetration into the recirculation region was at a minimum for these test conditions, actual fuel jet exit velocities for the conical nozzle were not established. The tests are therefore identified by overall air/fuel ratio. While not directly applicable to other geometries, the air/fuel ratio serves as a useful index for test condition identification and was, in fact, not found to be a significant parameter over the range studied.

## Experimental Results

### Mean Flowfields

Vector plots for the test fuel conditions are shown in Figs. 2–7. The uncertainty in each component of the mean velocities, as obtained from a series of measurements at a fixed location and fuel rate, is approximately 0.25 m/s.

The flow pattern in this type system has been postulated by Chen and Lightman,<sup>6</sup> Roquemore et al.,<sup>7</sup> and Roquemore et al.<sup>8</sup> At low heat release rates, the pattern looks as expected with a single recirculation vortex between the fuel nozzle and the centerbody outer radius and no significant flow across the burner centerline. This matches the referenced anticipated results.

Figure 2 shows the flow pattern with no flow through the fuel nozzle. The recirculation pattern downstream of the centerbody face is clearly evident with a centerline stagnation point at approximately  $x/R=1.8$  and a circulating flow centered around a point near ( $x/R=0.75$ ,  $r/R=0.6$ ) in the separated zone. The presence of a small velocity component normal to the centerline indicates that the flow is not completely symmetric. Since the direction and magnitude of this centerline component was generally consistent throughout the

tests, it is believed to be the result of a nonuniform distribution of air into the supply chamber feeding the annular air passage. At the outer radius of the centerbody ( $r/R=1$ ), the velocity approaches the annular average of 14 m/s. The mean flow has become fairly uniform by four radii downstream.

Figure 3 shows the effect of injecting nitrogen at an  $a/f$  mass ratio of 400. The centerline velocity at  $x/R=0.50$  drops somewhat due to the influence of the fuel jet, and there is some increase in radial outflow along the centerbody face, suggesting that the fuel jet reverses in less than 0.5 radii and flows radially outward along the face of the centerbody to be entrained in the axially outflowing air in the shear layer near  $r/R=0.9$ . No attempt was made to specifically locate the fuel jet stagnation point.

This characteristic of the fuel jet flow corresponds to the type A pattern of Masri and Bilger<sup>9</sup>; although the apparatus used in the present study displayed this behavior at calculated jet velocities as high as 47 m/s in reacting flows and 63 m/s for the nonreacting nitrogen flow, whereas the referenced results would indicate a maximum expected velocity for this pattern to be near 30 m/s. The configurations of the fuel nozzles were different, however, with theirs being a straight jet rather than the conical nozzle used for the current tests. Other than the local influences of the fuel jet near the centerbody face, differences between the two nonreacting cases are negligible and the recirculation length in the axial direction stays constant at 1.8 radii. For the burner used in this test, the transition to other flow patterns, such as cases where the fuel jet dominates the centerline flow and does not stagnate and reverse, were not investigated.

Figure 4 depicts the flowfield with a propylene fuel at  $a/f=6000$ , which is about the maximum value (or lean limit) at which combustion can be maintained in this burner. Even this relatively small amount of heat release can be seen to increase radial outflow near the face, increase axial inflow throughout the recirculation zone, expand the recirculation region radially, and lengthen the recirculation axially to 2.2 radii. Schefer et al.<sup>5</sup> observed a similar shift of this downstream stagnation point. Due to the radial expansion, the position of the zero axial velocity surface has shifted. The significance of this surface, as pointed out by Switzer et al.,<sup>10</sup> is that it separates the gases flowing axially outward from the recirculated gases flowing axially inward, with significantly different histories for the fluid elements on either side. It is seen that the effect of a small amount of heat release is more significant than the fluid mechanical effect of a nonreacting fuel jet even at nearly 15 times the mass flow, for the range of conditions tested.

The vector plots provide more insight into the effects of varying heat release rate and fuel chemistry. Isobutene at  $a/f=800$  (see Fig. 5) and a 1:1 mixture of butene and nitrogen at overall  $a/f=400$  (including the nitrogen diluent, see Fig. 6) have approximately the same heat release per unit time with the latter having twice the fuel jet mass flow. In this case, the fluid mechanical effect of the higher jet velocity can be seen in the radial outflow on and near the centerline at  $x/R=0.5$ . There is also some shift in the vectors along the recirculation region/annular flow shear layer, but this variation is probably within the positioning accuracy of the burner table mechanism as the velocity gradient is very high in this region. The patterns are otherwise quite similar.

A comparison between butene/nitrogen 1:1 mix and butene/nitrogen 2:1 mix (see Fig. 7) shows no significant difference. Here the heat release changes by 50% at a fixed fuel-mass flow. Both patterns are seen to be quite similar to the propylene flowfield at  $a/f=6000$ . At the higher heat release rates within this group (see Figs. 5–7), increased radial inflow (or decreased outflow) near the shear zone near  $r/R=0.8$  indicates a slight radial expansion of the recirculation zone, but no axial change is evident as the centerline stagnation point holds constant at 2.2 radii. The general trend shows no significant change in flow pattern or recirculation zone extent

despite a ten-fold increase in fuel flow. It is again observed that fuel jet flow rate is not a strong driver of flowfield pattern within the range tested. It also seems that the effect of heat release is most dramatic at very low fuel rates, with increasing fuel flow not being significant to the structure of the recirculation zone. The specific fuel chemistry, as expected, shows no influence on the flowfield. Lower air/fuel ratio tests were attempted, but the associated high soot loadings created significant data acquisition difficulties.

#### Turbulent Fluctuations

An evaluation of the turbulent fluctuation levels was conducted for the cases of no fuel jet, the nonreacting nitrogen fuel jet, and the propene-fueled results at  $a/f = 6000$ . These results can be compared to the limited data from similar, centerbody-type experiments and also to typical premixed studies. The rms averaged fluctuations are accurate to approximately 0.15 m/s, are TBD weighted, and have been calculated from three-sigma-filtered velocity files.

Figure 8 depicts the rms deviation in the radial velocity component ( $v'$ ) for these cases. The data from the nitrogen test and the test with no fuel jet match within the experimental accuracy at 42 of the 45 points in the spatial matrix; therefore only the nitrogen and propene results are plotted. The points for the propene flame have been connected to serve as a reference line for the other data. For the two cases, little influence of the fuel jet or reaction is seen as the curves for the different fuel conditions match closely. Independent of the fuel effects, other general trends are apparent. The turbulent velocities in the recirculating region are higher than in the mainstream and are higher near the centerline at large  $x/R$  than in the areas closer to the burner face. This means that the turbulent fluctuations originally present in the annular flow region increase in the separated portion of the flow as it turns and begins flowing radially and axially inward. This level then diminishes as the flow travels down (axially inward) along the centerline and then radially outward along the face of the centerbody. There is no indication that the reaction greatly af-

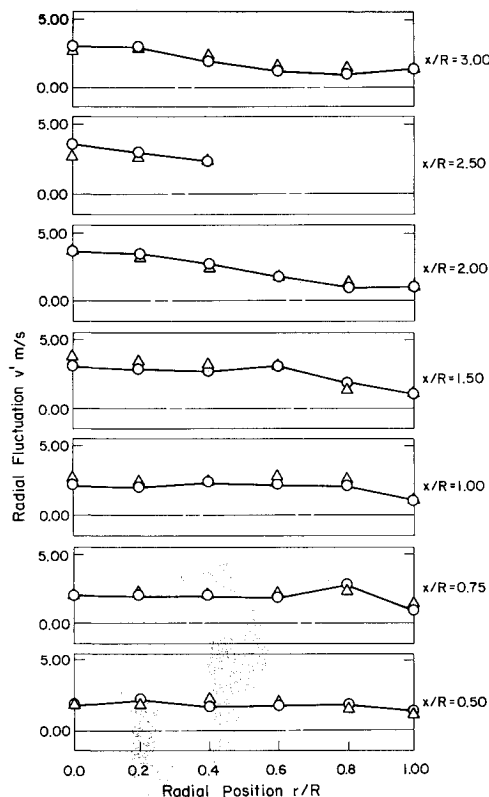


Fig. 8 Radial profiles of radial turbulence component at seven axial locations (—○— propene,  $a/f = 6000$ , —△— nitrogen,  $a/f = 400$ ).

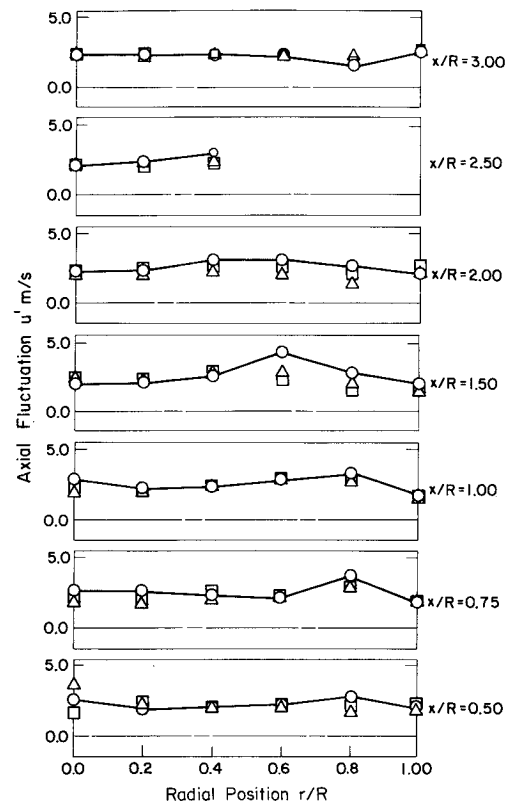


Fig. 9 Radial profiles of axial turbulence component at seven axial locations (—○— propene,  $a/f = 600$ , —△— nitrogen,  $a/f = 400$ , —□— no fuel jet).

fects the radial turbulent component within the recirculation zone.

Figure 9 shows different trends for the axial fluctuations ( $u'$ ). The fluctuations are still somewhat higher in the recirculation region than in the inlet flow, but the presence of reaction can be seen to increase the turbulence in the flow immediately downstream of the flame front even at this lean condition. This additional contribution to the fluctuations diminishes rapidly, however, with no indication of the reaction influence seen by axial position  $x/R = 3.0$ . At the position nearest the fuel nozzle exit, the fluctuations correlate well with the fuel jet flow rate with the highest turbulence for the nitrogen jet at  $a/f = 400$  and the lowest for the no-fuel condition.

Switzer et al.<sup>10</sup> obtained axial statistics in a centerbody burner similar to that used in this study and also showed a fluctuation increase near the flame front and axial turbulence levels on the order of 20% relative to the annular inlet velocity. This magnitude agrees closely with the present work. Schefer et al.<sup>5</sup> observed a similar increase in  $u'$  with reaction.

In the nonreacting, separated flow in a disk wake, Durao and Whitelaw<sup>14</sup> observed that, near the centerline stagnation point, the radial fluctuations were as much as 100% higher than the axial fluctuations. A comparison between Figs. 8 and 9 shows a similar trend seen at  $x/R = 1.50$  and  $x/R = 2.00$  in both reacting and nonreacting cases; although the increase of the radial over the axial turbulence is more on the order of 75%. An examination of the referenced radial profiles showed an increase in axial fluctuations with increasing radius; whereas the present results show a more constant turbulence with a peak near the annular/recirculated mixing layer. Radial fluctuations were constant in the referenced work, and a radially decreasing trend is seen in Fig. 8. The substantially nonisotropic nature of the turbulence in the separated region is inconsistent with  $k-\epsilon$  modeling and must be considered when closure models are applied.

The observation that the axial turbulence is influenced more heavily by the reaction is consistent with the results of Moreau

and Boutier<sup>15</sup> in premixed flames in a duct. Cheng and Ng<sup>16</sup> observed sharp increases in both fluctuating components in the reaction zone in a rod-stabilized, premixed flame; Yoshida<sup>17</sup> saw no major change in turbulence at the flame front in a Bunsen flame. The major source of discrepancy in these studies is the specific geometry tested. The characteristics of the flame front that would be expected to alter the observed fluctuations include wrinkling, intermittency, steadiness, and the angle between the flame front and the instantaneous velocity vector. Generally, the reaction can be expected to accelerate the flow due to expansion, and the component of velocity more nearly normal to the flame front would be expected to show the higher fluctuations. In addition, the volumetric energy release rate will differ greatly between premixed and nonpremixed cases—especially at fuel-lean conditions such as studied here. Conclusions from differing test geometries and heating rates must be interpreted with these considerations.

### Turbulence Correlations

The most apparent effect of the reaction is seen in the shear stress distribution. Figure 10 shows that the Reynolds shear ( $-\overline{uv}$ ) is generally slightly negative along the centerline. The stress then turns to the positive in the recirculating zone but shows a marked increase in the vicinity of the reaction front, which also coincides with the high velocity gradient region where the outer radius of the recirculating pattern merges with the annular flow.

This increase in shear then dissipates downstream in a manner similar to the axial fluctuation. It can also be seen that the shear stress decreases as the flow turns and starts back down in the recirculating part of the flow which indicates a nonrandom correlation originating in the high-mean velocity gradient region of the flow (with a higher Reynolds stress seen in the reacting case) and decaying as the flow recirculates. This decay occurs faster in the reacting case than in the nonreacting flowfields.

It should also be noted that although the low shear zones observed at  $x/R=0.50, 0.75$ , and 1 generally correspond to areas of low velocity gradient, the turbulence levels in these regions are substantial. Areas of zero shear do not generally correspond to areas of zero turbulent kinetic energy. These facts are not consistent with eddy-viscosity modeling schemes. Concerning general trends in the relations, the data for no fuel jet generally match the nonreacting nitrogen fuel jet data more closely than the reacting case, again, indicating the predominance of energy release effects over purely fluid mechanical influences. The maximum shear is approximately 2.5% of the squared inlet velocity, which compares closely with the nonreacting results of Leder<sup>18</sup> behind a flat plate with a splitter and is an order of magnitude lower than Leder's value behind the same plate without a splitter in the separated flow region. Moreau and Boutier<sup>15</sup> observed no significant shear stress in their evaluation, Yoshida<sup>17</sup> noted a slight increase in shear through the reacting region, and Cheng and Ng<sup>16</sup> saw a sharp increase, all of these in premixed, reacting systems. The geometry arguments which apply to the interpretation of the individual turbulent components also apply to the cross correlations. Durao and Whitelaw<sup>14</sup> show low shears near the centerline, then positive in the recirculation zone, and negative downstream. This shows some agreement; although the referenced data show an earlier transition to negative values and much larger areas of negative shear. These results are also qualitatively similar to those of Schefer et al.<sup>5</sup> with the highest shears, as expected, in the boundary region between the recirculating region and annular flow and the shear distribution broadening in the downstream areas.

Other evidence of the extent of correlation between the velocity fluctuations is indicated in Fig. 11. The correlation coefficient  $-\overline{uv}/(\overline{u'u'}\overline{v'v'})$  is seen to have a fairly low magnitude along the centerline and in the unseparated regions which are dominated by undisturbed flow from the annulus. This is in-

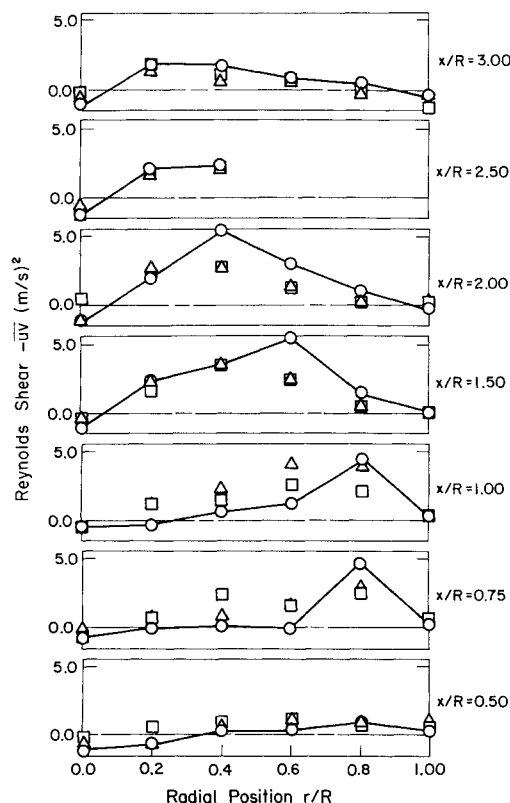


Fig. 10 Radial profiles of Reynolds shear stress at seven axial locations (—○— propene,  $a/f=6000$ , —△— nitrogen,  $a/f=400$ , —□— no fuel jet).

dicative of generally random, or uncorrelated, turbulence, as also reflected by the low shear values in these areas. Within the recirculation zone, the coefficient trends to higher values, indicating some correlation to the turbulent fluctuations.

Although the effect of the reaction on this parameter is not strongly defined, there is some indication that combustion may increase the correlation near the flame front and in the immediate downstream regions, but some nonreacting flow regions show correlations nearly as high as the maximum value of 0.5 observed in the reacting case. The uncertainty level for the correlation coefficient is relatively high due to accumulation of errors in the three terms used for its calculation making strong arguments from this presentation of the data difficult to make.

The indicated increase in correlation near the reaction zone may be partially a result of flame front intermittency, where motion of the flame front would influence the flow in a manner exhibiting high correlation, but more akin to unsteady flow than to small-scale turbulence. An inspection of time-dependent shear in the high correlation area near the flame front indicated a fairly random nature with no obvious periodicity that might be associated with flame-front motion. The observed correlation in this region cannot be entirely attributed to the presence of the reaction as the nonreacting cases show somewhat the same trend—although to a lesser degree.

The maximum correlation of 0.5 is consistent with the results of Schefer et al.<sup>5</sup> and is not indicative of highly correlated fluctuations. Cheng and Ng<sup>16</sup> measured values as high as 0.75 near the flame front in a rod-stabilized, premixed flame with the correlation coefficient reaching above 0.95 along the centerline of the wake. A recalculation of Yoshida's data<sup>17</sup> produces correlation coefficients ranging from 0.28 to 0.20 with the highest value seen just downstream of the flame front of the Bunsen burner. The extent of correlation must also be interpreted considering the limits imposed by the correlation window in the data interface. The 1.2 milliseconds processor coincidence time in effect for these experiments will

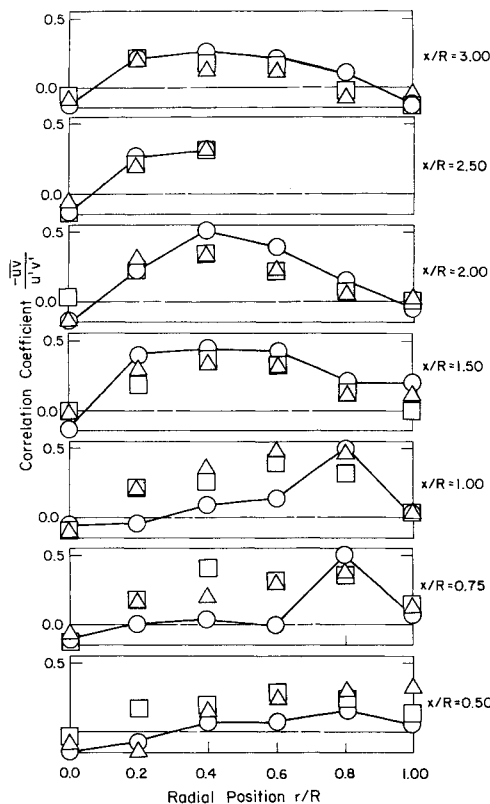


Fig. 11 Radial profiles of correlation coefficient at seven axial locations, symbol size represents uncertainty (—○— propene,  $a/f = 6000$ , —△— nitrogen,  $a/f = 400$ , —□— no fuel jet).

randomize turbulence correlations occurring over shorter time scales; therefore the results presented should only be seen as indicative of trends in large-scale, low-frequency fluctuations. If the radius of the centerbody is taken as the relevant scale length, a reference velocity of 14 m/s corresponds to a characteristic flow frequency of approximately 500 Hz which implies that the coincidence time used should identify any large-scale fluctuations present.

### Conclusions

The separated, reacting flowfield in the wake of a centerbody diffusion burner was mapped using a two-component LDA system. The following conclusions can be drawn:

a) TBD-weighted mean velocities and turbulence fluctuations did not significantly vary from particle averages.

b) The mean-flow patterns were found to be in agreement with the qualitative predictions of other researchers. The fuel flow stagnates quickly downstream of the nozzle and flows radially outward along the centerbody face where it continually mixes with the recirculating vortex gases and begins reacting.

c) For the range of fuel flows tested, the fluid mechanical effect of the centerline fuel jet was found to be not a significant contributor to the overall flow pattern. Likewise, fuel chemistry did not influence the mean flowfield. The effect of heat release was found to be most significant when comparing nonreacting flows to flows with low heat release; the addition of fuel beyond the minimum required to sustain combustion did not substantially alter the mean flowfield.

d) The turbulence in the separated region was found to be nonisotropic. The presence of reaction has no significant influence on radial turbulence but increases the axial level near the reaction region. Near the centerline stagnation point, the radial fluctuations are 75% greater than the axial fluctuations in both reacting and nonreacting cases. The average Reynolds shear is relatively low with an increase near the flame front in reacting flows.

e) The nonisotropic nature of the turbulence and the observed occurrence of zero shear in regions of nonzero turbulent kinetic energy are generally inconsistent with eddy viscosity and  $k-\epsilon$  turbulence models.

### Acknowledgment

The research on which this document is based was funded in part by the U. S. Air Force, Air Force Engineering and Services Center, Tyndall Air Force Base, Florida, and in part by the College of Engineering of the University of Florida.

### References

- <sup>1</sup>Hinze, J. O., *Turbulence*, 2nd ed., McGraw-Hill, New York, 1975, p. 4.
- <sup>2</sup>Edwards, R. V., ed., "Report of the Special Panel on Statistical Particle Bias Problems in Laser Anemometry," *ASME Journal of Fluids Engineering*, Vol. 109, No. 2, June 1987, pp. 89-93.
- <sup>3</sup>Proctor, C. L., II, Beladi, S. E., Roe, L. A., and Touati, A., "Optical Measurement of Flame Structure and Soot Emissions," University of Florida Combustion Laboratory, Gainesville, FL, USAF Contract F08635-C-0136, Task Order 83-03, 1985.
- <sup>4</sup>Lightman, A. J., Richmond, R. D., Krishnamurthy, L., Magill, P. D., Roquemore, W. M., Bradley, R. P., Jr., Stutrud, S., and Reeves, C. M., "Velocity Measurements in a Bluff-Body Diffusion Flame," AIAA Paper 80-1544, July 1980.
- <sup>5</sup>Schefer, R. W., Namazian, M., and Kelly, J., "Velocity Measurements in a Turbulent Nonpremixed Bluff-Body Stabilized Flame," AIAA Paper 87-1349, June 1987.
- <sup>6</sup>Chen, T. H. and Lightman, A. J., "Effects of Particle Arrival Statistics on Laser Anemometer Measurements," *International Symposium on Laser Anemometry*, ASME, FED, Vol. 33, New York, 1985, pp. 231-234.
- <sup>7</sup>Roquemore, W. M., Bradley, R. P., Stutrud, J. S., Reeves, C. M., and Krishnamurthy, L., "Preliminary Evaluation of a Combustor for Use in Modeling and Diagnostics Development," ASME Paper 80-GT-93, March 1980.
- <sup>8</sup>Roquemore, W. M., Bradley, R. P., Jackson, T. A., Kizirnis, S. W., Goss, L. P., Switzer, G. L., Trump, D. D., Sarka, B., Ballal, D. R., Lightman, A. J., Yaney, P. P., and Chen, T. H., "Development of Laser Diagnostics for Combustion Research," Spring Technical Meeting of the Central States Section of the Combustion Institute, Cleveland, May 1986.
- <sup>9</sup>Masri, A. R. and Bilger, R. W., "Turbulent Diffusion Flames of Hydrocarbon Fuels Stabilized on a Bluff Body," *Twentieth Symposium (International) on Combustion*, The Combustion Institute, Pittsburgh, 1985, pp. 319-326.
- <sup>10</sup>Switzer, G. L., Goss, L. P., Trump, D. D., Reeves, C. M., Stutrud, J. S., Bradley, R. P., and Roquemore, W. M., "CARS Measurements in the Near-Wake Region of an Axisymmetric Bluff-Body Combustor," *AIAA Journal*, Vol. 24, No. 7, July 1986, pp. 1155-1162.
- <sup>11</sup>Lightman, A. J. and Magill, P. D., "Velocity Measurements in Confined Dual Coaxial Jets Behind an Axisymmetric Bluff Body: Isothermal and Combusting Flows," Air Force Wright Aeronautical Labs, AFWAL-TR-81-2018, 1981.
- <sup>12</sup>Proctor, C. L., II, Roe, L. A., and Touati, A., "Optical Measurement of Soot Formation," U. S. Air Force/University of Florida Combustion Laboratory, Gainesville, FL, 1987 (to be published as AFESC TR).
- <sup>13</sup>Touati, A., "Investigation of Soot Formation in a Bluff Body Stabilized Flame," Ph.D. dissertation, University of Florida, 1987.
- <sup>14</sup>Durao, D. F. G. and Whitelaw, J. H., "Velocity Characteristics in the Near Wake of a Disk," *Journal of Fluid Mechanics*, Vol. 85, Part 2, March 1978, pp. 369-385.
- <sup>15</sup>Moreau, P. and Boutier, A., "Laser Velocimeter Measurements in a Turbulent Flame," *Sixteenth Symposium (International) on Combustion*, The Combustion Institute, Pittsburgh, Pa., 1976, pp. 1747-1756.
- <sup>16</sup>Cheng, R. K. and Ng, T. T., "Velocity Statistics in Premixed Turbulent Flames," *Combustion and Flame*, Vol. 52, Sept. 1983, pp. 185-202.
- <sup>17</sup>Yoshida, A., "An Experimental Study of Wrinkled Laminar Flame," *Eighteenth Symposium (International) on Combustion*, The Combustion Institute, Pittsburgh, Pa., 1980, pp. 931-939.
- <sup>18</sup>Leder, A., "Physical Properties of Separated Flows Behind Two-Dimensional Bluff Bodies in Uniform Flows," *International Symposium on Laser Anemometry*, ASME, FED, Vol. 33, New York, 1985, pp. 273-280.